

# Erdheim-Chester disease with rare radiological features in a 14-year old girl with pre-B Acute Lymphocytic Leukemia and Diabetes mellitus

Varanasi Venkata Rama Krishna<sup>1\*</sup>, Teo Eu Leong Harvey James<sup>1</sup>,  
Kenneth Tou En Chang<sup>2</sup>, Soh Shui Yen<sup>3</sup>

1. Department of Diagnostic Imaging, KK Women's and Children's Hospital, Singapore

2. Department of Pathology and laboratory medicine, KK Women's and Children's Hospital, Singapore

3. Department of Hematology and Oncology, KK Women's and Children's Hospital, Singapore

\* **Correspondence:** Varanasi Venkata Rama Krishna, Department of Diagnostic Imaging, KK Women's and Children's Hospital, 100, Bukit Timah Road, Singapore 229899, Singapore  
(✉ [vvrk67@hotmail.com](mailto:vvrk67@hotmail.com))

Radiology Case. 2014 Aug; 8(8):7-15 :: DOI: 10.3941/jrcr.v8i8.1899

## ABSTRACT

We report a case of a 14 year-old girl with Diabetes Mellitus who was in remission with pre-B cell Acute Lymphoblastic Leukemia and subsequently diagnosed with Erdheim-Chester disease. Erdheim-Chester disease is a non-Langerhans cell histiocytosis and is very rare in children. In addition, the radiological features of the lesions are atypical and have not been reported in children. There is no known association between the three conditions and this is the first reported case in the literature. A literature review of Erdheim-Chester disease will be performed.

## CASE REPORT

### CASE REPORT

A 14-year-old female with pre-existing Type 2 Diabetes Mellitus (DM) controlled with metformin and who was in remission for pre-B cell Acute Lymphoblastic Leukemia (ALL), presented with complaints of bilateral knee pain, lumps in her forehead and dorsum of the right hand. On clinical examination she was found to have soft tissue swellings over the scalp and forearm. Laboratory results notably the white blood cell count, C-reactive protein and Erythrocyte sedimentation rate were normal.

#### Imaging findings

Magnetic Resonance Imaging (MRI) of head was performed to evaluate the scalp lesions and to assess for intracranial involvement. Multiple focal osseous lesions were seen within the skull vault and bony orbit (Figure 1). Focal nodular thickening of the meninges was noted, with the largest nodule situated in tentorium cerebelli on the left side (Figure 1D). The brain parenchyma was normal. The bony lesions were isointense on T1WI, T2WI and showed mild homogeneous enhancement after the administration of intravenous Gadolinium.

Plain radiographs of skull, forearms and legs showed multiple well-defined osteolytic lesions without sclerosis ranging in size from 0.5 to 1.5cm (Figures 2 & 3). Some of the vault lesions were entirely intradiploic and some involved either the inner or the outer table only. The lesions involving only the outer table were associated with overlying soft tissue swelling. Similar lesions were seen in the radii, ulnae, femora, tibiae and fibulae. Technetium-99m bone scintigraphy revealed diffuse tracer uptake with a few other areas of increased uptake in the long bones (Figure 4).

An open biopsy of a skull vault lesion was performed. The biopsy specimen showed numerous large histiocytes with scattered multinucleate forms (including Touton-type), accompanying inflammatory cells comprising of lymphocytes, plasma cells and some neutrophils and eosinophils (Figure 5). The histiocytes had small round to oval nuclei lacking nuclear grooves or indentations and had abundant foamy cytoplasm. Some histiocytes contained red blood cells and leucocytes within the cytoplasm indicating erythrophagocytosis and leucophagocytosis respectively. The immunohistochemical stains showed positive staining for the histiocyte markers

CD68 and CD163 (Figure 6) and negative staining for S100 and CD1a. This is consistent with the diagnosis of Erdheim-Chester disease (ECD).

Computed Tomography (CT) of chest, abdomen and pelvis was performed for staging and it showed additional osteolytic lesions in the spine and the pelvic bone (Figure 7). The vertebral lesions varied from 0.4cm to 1.6cm in size. The largest lesion was in the C6 vertebral body extending to left pedicle with cortical erosion and an associated adjacent soft tissue component (Figure 7).

MRI of lower extremities showed more lesions than was seen on the plain radiographs. These lesions were seen in the diaphysis, metaphysis and epiphysis of the long bones. The femoral, tibial and fibular lesions were isointense to muscle on T1WI and hyper intense on T2WI with some enhancement after administration of Gadolinium (Figure 8 & 9).

#### Treatment & Follow up

The patient was treated with weekly Interferon alpha therapy. One year follow up radiographs showed stability of the previously noted osteolytic lesions (Figure 10) with no new lesions.

## DISCUSSION

### Etiology and Demographics

Erdheim-Chester disease (ECD) is a rare form of non Langerhans cell histiocytosis of unknown etiology [1]. It is distinct from Langerhans cell histiocytosis, presenting in fifth through seventh decades. Few hundreds of cases have been reported in the published literature [2]. There is slight male predominance of ECD in the largest series published by Veyssier-Belot C et al [3]. A review of English literature shows that only six cases have been reported in children with ages at diagnosis ranging from 7-14 years [1].

### Clinical and Imaging findings

The clinical presentation of patients with ECD varies depending upon the sites of involvement [3]. The classic triad of ECD is a combination of bone pain, Diabetes Insipidus and painless exophthalmos. Other symptoms include cerebellar syndrome, abdominal pain and skin xanthomas [3]. Most patients with ECD will have osseous involvement at the time of diagnosis and the vast majority will also have at least one non-osseous site of involvement. ECD may occasionally be detected incidentally in asymptomatic patients who have had radiographs performed for unrelated conditions [1].

The distinctive radiological feature of ECD is symmetrical sclerosis in the diaphysis of long bones [4]. Metadiaphyseal sclerosis, partial epiphyseal sclerosis, periostitis and focal pseudotumoral lesions have also been reported. These pseudotumoral lesions exhibit a variable degree of osteolysis, cortical destruction, and soft tissue masses [5, 6]. Osteolytic lesions, such as those seen in our case, are infrequent occurring in less than 10% cases [3]. In one of the case reports of ECD, osteolytic lesions were described in the spine and pelvis sparing the appendicular skeleton [5].

A unique feature in our patient is the presence of well-defined osteolytic lesions in the skeleton, with no osteosclerotic lesions. There are no reported cases of ECD in children presenting with lesions of this description.

ECD may involve extra-skeletal sites such as the retroperitoneum, retro-orbital region, brain, pituitary gland, skin, maxillary sinus, pericardium, large vessels, lungs and orbit [2,7]. Cardiac involvement can range from valve abnormalities; conduction defects to periaortic fibrosis along the entire course of vessel and is a significant source of morbidity and mortality. Pulmonary involvement is either of the pleura, the lung parenchyma, or both. Mediastinal infiltration, pleural thickening/effusion, centrilobular nodules, ground-glass opacities or lung cysts may be seen in CT of the lungs. Retroperitoneal involvement with ECD can manifest as a mass-like infiltrative lesion or as a rind-like lesion surrounding the kidneys. This can lead to acute or, more commonly, slowly progressive renal insufficiency. Percutaneous nephrostomy tubes are often required to alleviate ureteral obstruction. Skin involvement can occur as multifocal papulonodular lesions but is less common compared with LCH [3]. Central nervous system involvement is common in patients with ECD [2], with Diabetes insipidus being a common symptom when the pituitary is involved.

Histopathological analysis plays a key role in differentiating ECD from other types of histiocytosis. ECD differs from Langerhans cell histiocytosis in that the histiocytes in ECD demonstrate stain positively for CD68 and CD163 but do not stain for CD1A, S-100 protein and OKT6 which are seen in LCH [7, 8].

### Treatment & prognosis

A standard treatment regimen has not yet been established. Treatment with Interferon alpha 2 is preferred for newly-diagnosed symptomatic patients [2]. Patients are clinically assessed every three to six months. Affected organs should be imaged every three to six months until stability is documented. The frequency of imaging is determined by the baseline disease status, organ of involvement and requirement for ongoing treatment.

### Differential diagnosis

Each manifestation of ECD has its own differential diagnosis. Differential diagnosis based on osteolytic lesions in children includes Langerhans cell histiocytosis, infection, metastases from neuroblastoma and the differentiation is done by biopsy. In adults the differential diagnosis for osteosclerotic lesions includes Paget's disease, sclerotic myeloma associated with POEMS syndrome and metastases. Lack of symmetrical osteosclerosis is usually helpful in their differentiation; however a biopsy is essential to confirm the diagnosis.

In summary, our case is highly unusual in that ECD occurred in a young adolescent girl who had pre-existing diabetes mellitus and was in remission for pre-B ALL. These associations have not been previously described in the literature. Furthermore, the radiological features of the lesions were atypical in that they were well-defined osteolytic lesions

rather than the typical bilateral symmetrical ill-defined areas of sclerosis seen in the long bones.

TEACHING POINT

ECD disease is a form of non-Langerhans cell histiocytosis generally presenting in the fifth through seventh decades and is rare in children. Bone involvement is nearly universal with bilateral symmetric osteosclerosis of long bones being the typical radiological feature.

REFERENCES

1. Song SY, Lee SW, Ryu KH, Sung SH. Erdheim-Chester disease with multisystem involvement in a 4-year-old. *Pediatr Radiol.* 2012 May; 42(5):632-5. PMID:21879308
2. Haroche J, Arnaud L, Cohen-Aubart F et al. Erdheim-Chester disease. *Rheum Dis Clin North Am.* 2013 May; 39(2):299-311. PMID:23597965
3. Veysier-Belot C, Cacoub P, Caparros-Lefebvre D et al. Erdheim-Chester disease. Clinical and radiologic characteristics of 59 cases. *Medicine(Baltimore)* 1996 May; 75(3):157-69. PMID:8965684

4. Resnik D, Greenway G, Genant H, Brower A, Haqiqhi P, Emmett M. Erdheim-Chester disease. *Radiology* 1982 Feb; 142(2):289-95. PMID: 7054816
5. Klieger MR, Schultz E, Elkowitz DE, Arien M, Hajdu SI. Erdheim-Chester disease: a unique presentation with multiple osteolytic lesions of the spine and pelvis that spared the appendicular skeleton. *AJR Am J Roentgenol.* 2002 Feb; 178(2):429-32. PMID:11804910
6. Dion E, Graef C, Miquel A et al. Bone involvement in Erdheim-Chester disease: imaging findings including periostitis and partial epiphyseal involvement. *Radiology.* 2006 Feb; 238(2):632-9. PMID: 16371583
7. Drier A, Haroche J, Savatovsky J et al. Cerebral, facial, and orbital involvement in Erdheim-Chester disease: CT and MR imaging findings. *Radiology.* 2010 May; 255(2):586-594. PMID 20413768
8. Sheu SY, Wenzel RR, Kersting C, Merten R, Otterbach F, Schmid KW. Erdheim-Chester disease: case report with multisystemic manifestations including testes, thyroid, and lymph nodes, and a review of literature. *J Clin Pathol.* 2004 Nov; 57(11):1225-8. PMID 15509691

FIGURES

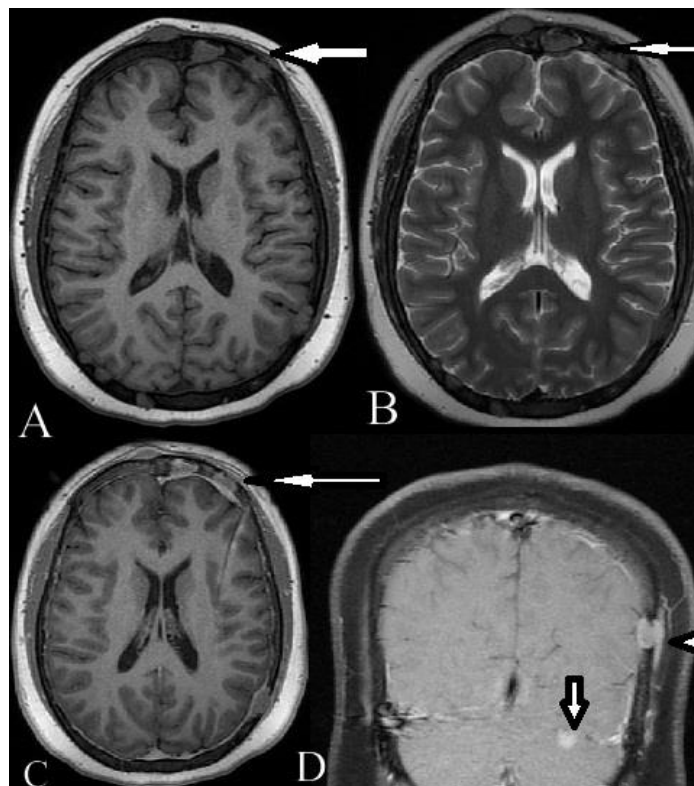


**Figure 1:** A 14 year old girl with Erdheim-Chester disease. MRI of the brain shows focal intermediate signal lesions in the vault (arrows) on T1WI (A) and T2WI (B). Post contrast axial (C) and coronal images (D) show homogeneous enhancement of vault lesions. In addition, the coronal image (D) also shows a focal enhancing lesion involving the tentorium cerebelli on left side (arrow). Technique: 1.5 T GE Signa HDXT scanner. Image A) Axial Fast spin echo T1WI TR/TE9.38/3.74, slice thickness/Interval 2/0.99. Image B) Axial Fast spin echo T2WI TR/TE 4520/105.312, slice thickness/Interval 5/7. Images C & D) Contrast enhanced axial(C) coronal (D) Fast spin echo T1 WI TR /TE 9.34/3.72, slice thickness/Interval 2/0.99. 10 ml of Gadolinium based contrast agent (Dotarem) was administered intravenously.

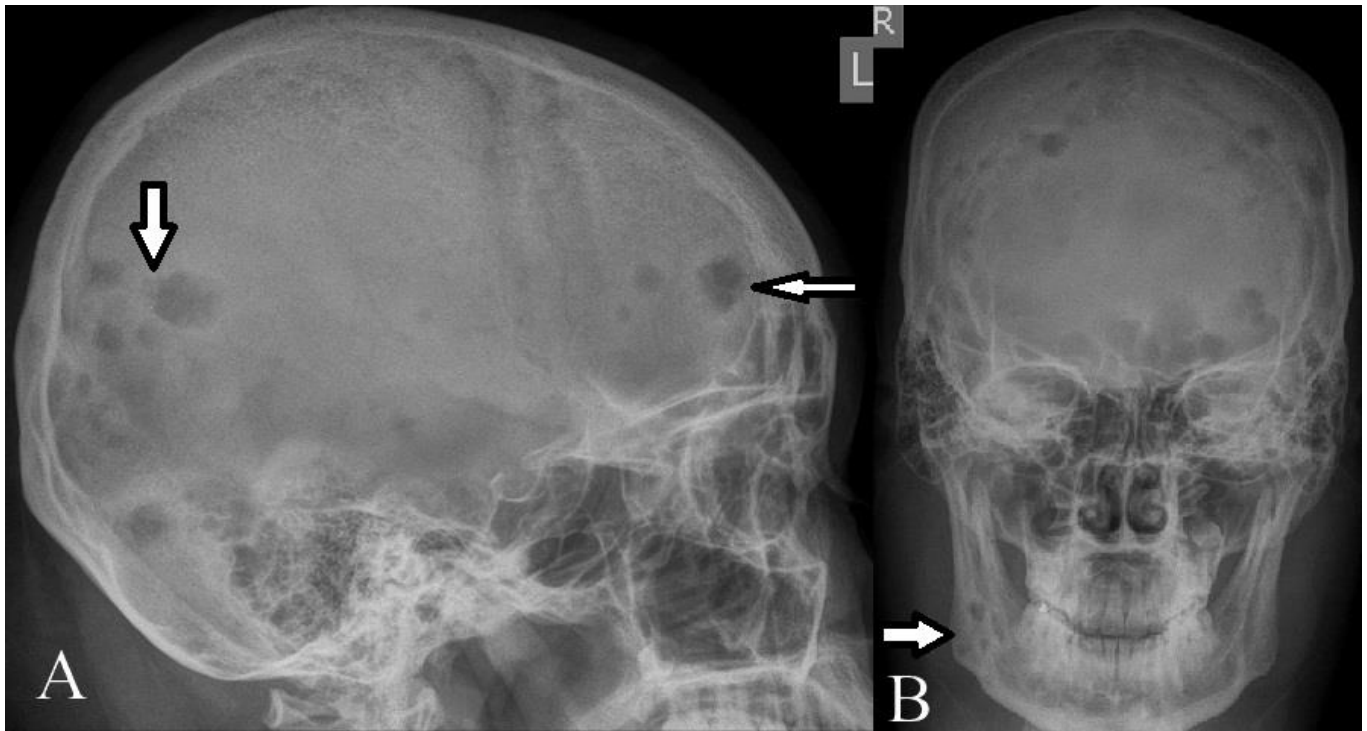


**Figure 2:** A 14 year old girl with Erdheim-Chester disease. Plain radiographs of skull, lateral view (A) and AP view (B) show multiple osteolytic lesions in the vault involving the frontal, parietal bones (arrows) and the mandible (arrows). There is no perilesional sclerosis.

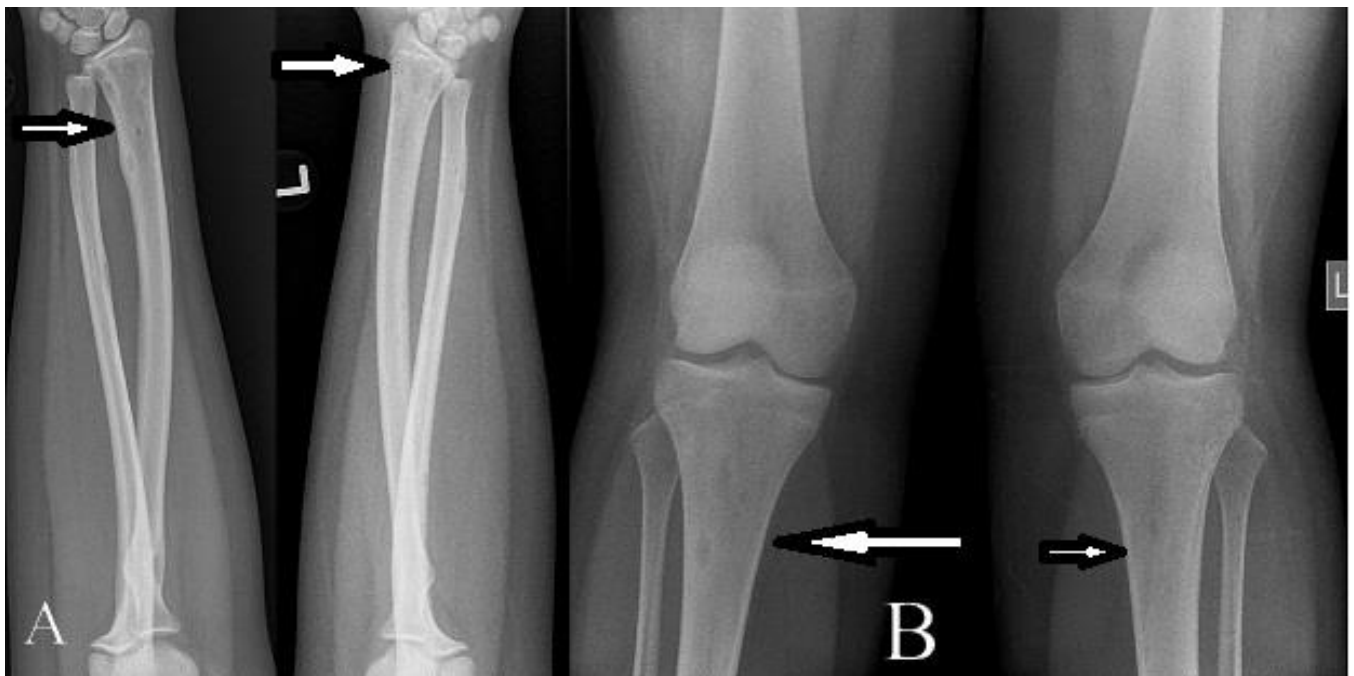


**Figure 3:** A 14 year old girl with Erdheim-Chester disease. Plain radiographs of fore arm (A) show well defined osteolytic lesions in the distal radial, ulnar metaphyseal regions (arrows). Plain radiograph of both knees frontal view (B) shows small well defined osteolytic lesions in proximal metaphyseal and diaphyseal regions of tibiae (arrows). Note the absence of sclerotic lesions in distal femora.

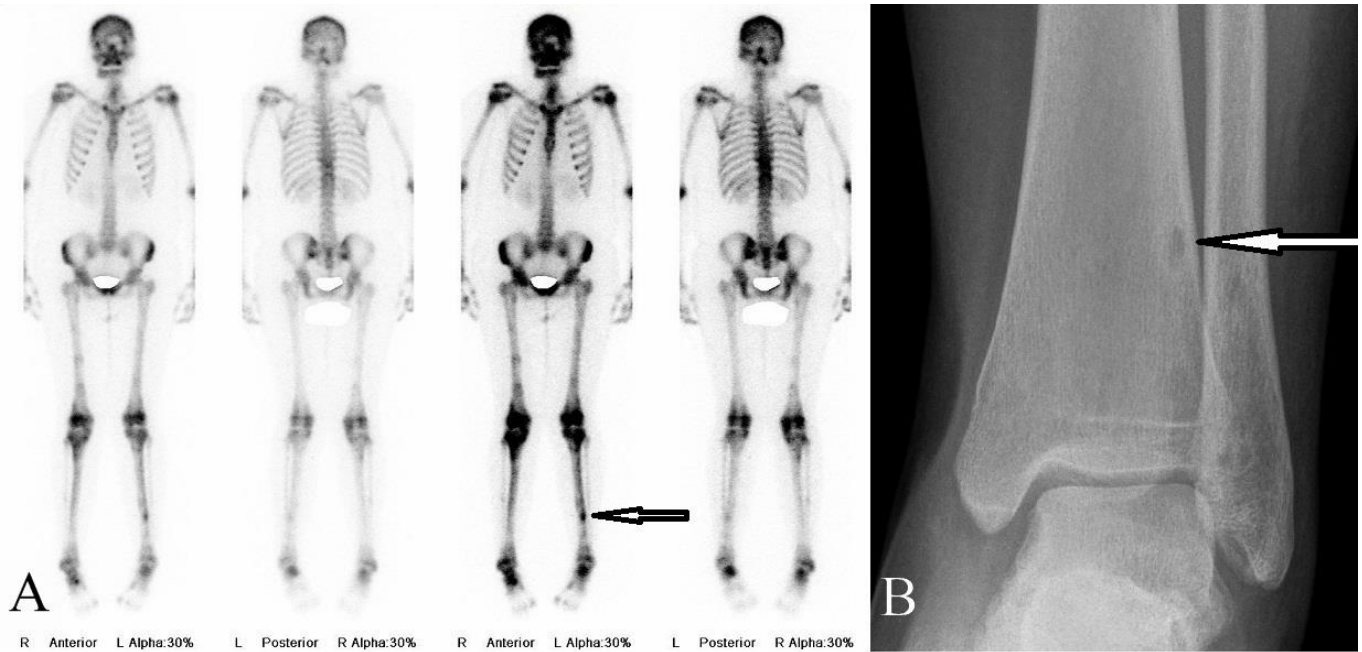


**Figure 4:** A 14 year old girl with Erdheim-Chester disease.

A) Tc 99m MDP bone scan delayed image shows diffuse tracer uptake with focal increased tracer uptake in long bones, as in left distal tibial diaphysis (arrow).

B) Plain radiograph of left ankle and distal leg shows the osteolytic lesion in distal tibia (white arrow) corresponding to the increased tracer uptake on bone scan. The Fig 3B shows proximal tibial osteolytic lesions.

Technique: Delayed images of bone scintigraphy were obtained three hours after intravenous injection of 873 Mbq dose of Tc 99mMDP to the patient.

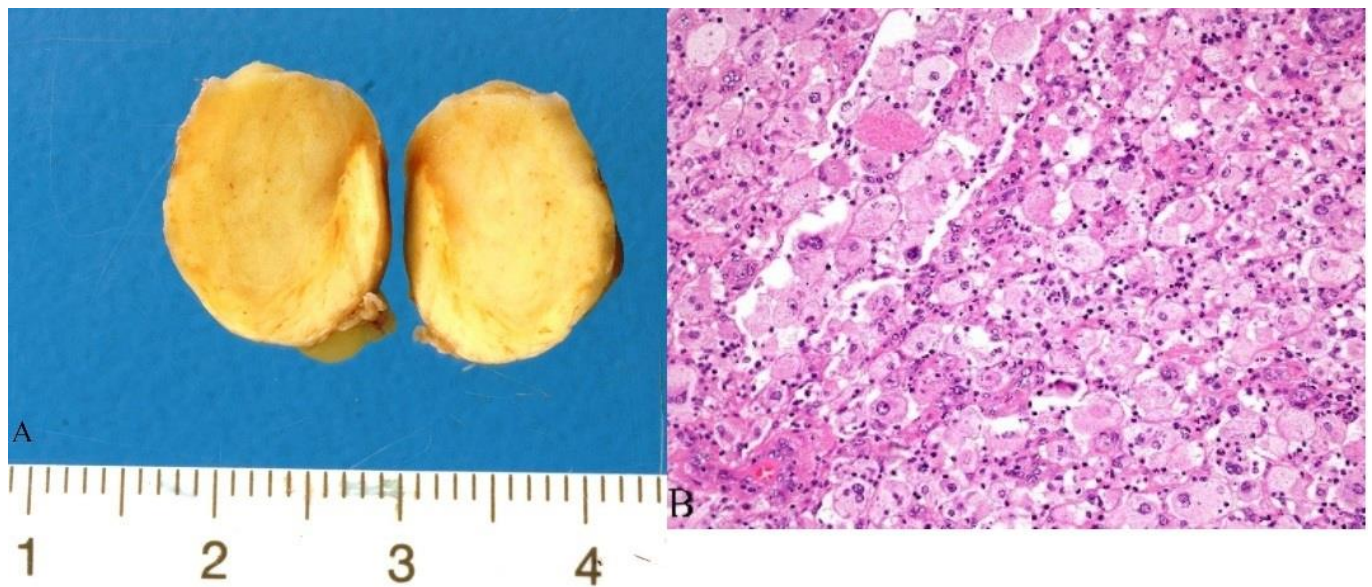


**Figure 5:** A 14 year old girl with Erdheim-Chester disease.

Photograph of resected left parietal bone lesion/ nodule (A) shows solid yellow cut surface with no necrotic, fleshy or cystic areas.

Hematoxylin and eosin -stained photomicrograph (B) shows sheets of large histiocytes and accompanying inflammatory cells. The histiocytes have small round to oval nuclei lacking nuclear grooves or indentations, and abundant foamy cytoplasm.

Technique: Hematoxylin &Eosin stain with high power (magnification x 200)

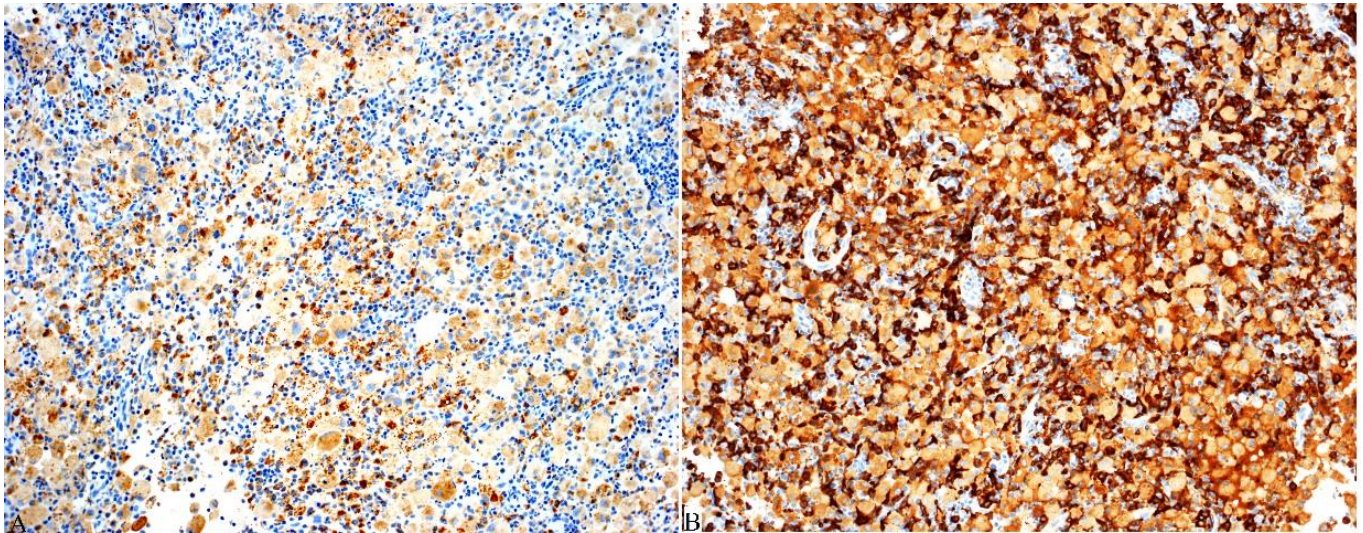


**Figure 6:** A 14 year old girl with Erdheim-Chester disease. Immunohistochemical staining shows the histiocytes in the specimen expressing the histiocyte markers CD68 (A) and CD163 (B).

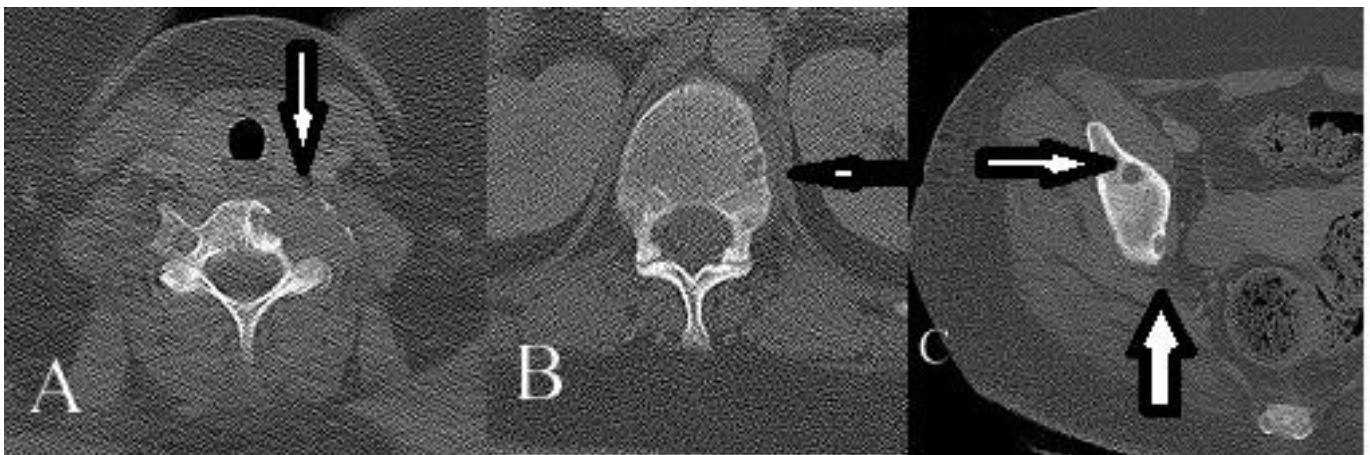


**Figure 7:** A 14 year old girl with Erdheim-Chester disease.  
 A) Axial computed tomography image of cervical spine at C6 level shows a lucent lesion in the vertebral body on left side extending to left pedicle (arrow) associated with soft tissue component (arrow).  
 B) Axial computed tomographic image of lower thoracic spine shows a lucent lesion in the vertebral body on left side (arrow).  
 C) Axial computed tomography image at the level of acetabulum shows lucent lesions in the right acetabulum (arrows).  
 Technique: Toshiba Aquilion 64 scanner, Slice thickness 5mm, Kvp120, mAs 101, Fov 500. Intravenous contrast administered: Omnipaque 300, volume 90ml.

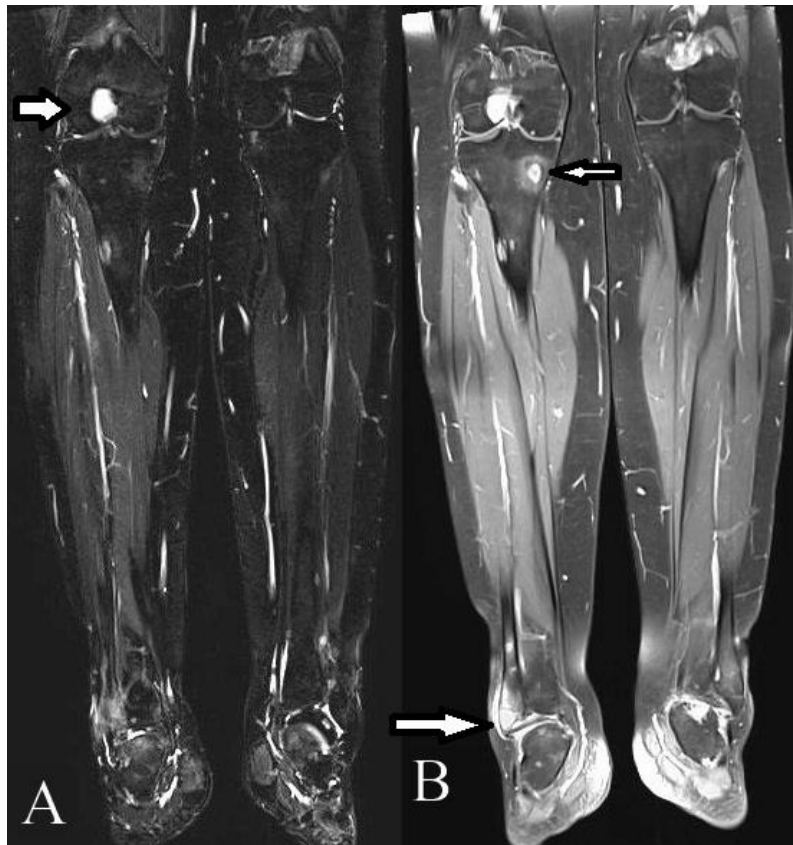


**Figure 8:** A 14 year old girl with Erdheim–Chester disease.

A. Coronal IR image of lower extremities shows more osseous lesions than on plain radiographs (arrows).

B. Coronal contrast enhanced T1 weighted image with fat saturation shows enhancing lesions in distal femoral epiphysal region, right proximal tibia and in right lateral malleolus (arrows).

Technique: MR images acquired on 3T Siemens SKYRA scanner. IR images were acquired with parameters of TR/TE 4500/68, TI 230ms. Slice thickness/Interval 5.19/5.2. T1Weighted images were obtained after intravenous administration of 10 ml. of Gadolinium (Dotarem) (TR/TE 550/9.5) Slice thickness/Interval 5.5/6.05

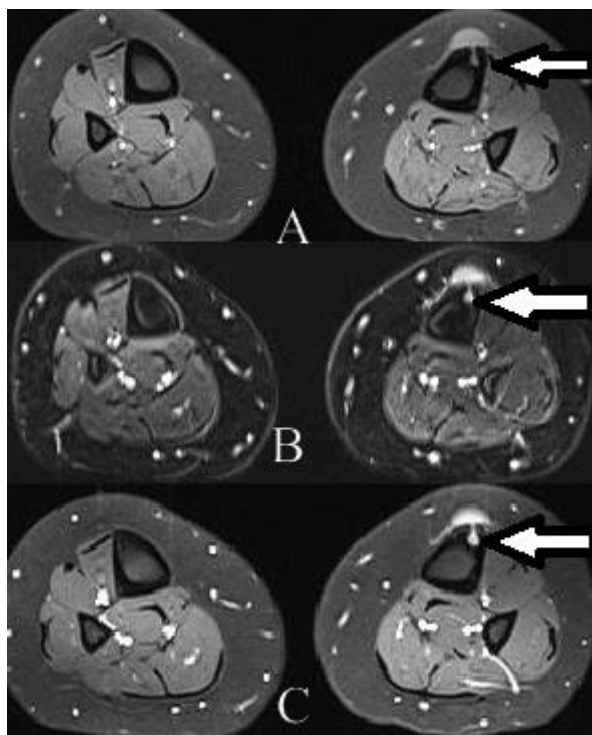


**Figure 9 (left):** A 14 year old girl with Erdheim–Chester disease. A,B,C) Axial images at lower third of legs shows an anterior cortical lesion in left tibia with adjacent soft tissue component (pseudotumoral lesion) . On T1 weighted fat saturated image (A) it is isointense to muscle. On T2 weighted fat saturated image (B) it is slightly hyper intense to the adjacent muscle. On post contrast T1 weighted fat saturated axial image(C), it shows mild homogeneous enhancement.

Technique: Magnetic Resonance Imaging was performed on 3.0 T Siemens SKYRA scanner, before and after injection of intravenous Gadolinium (10 ml. of Dotarem). Fast spin echo T1 Weighted (TR/TE 550/9.5) Fast spin echo T2 Weighted (TR /TE 6300/73) Post contrast T1 Weighted (TR /TE 6300/73) axial images. Slice thickness/Interval 5.5/6.05

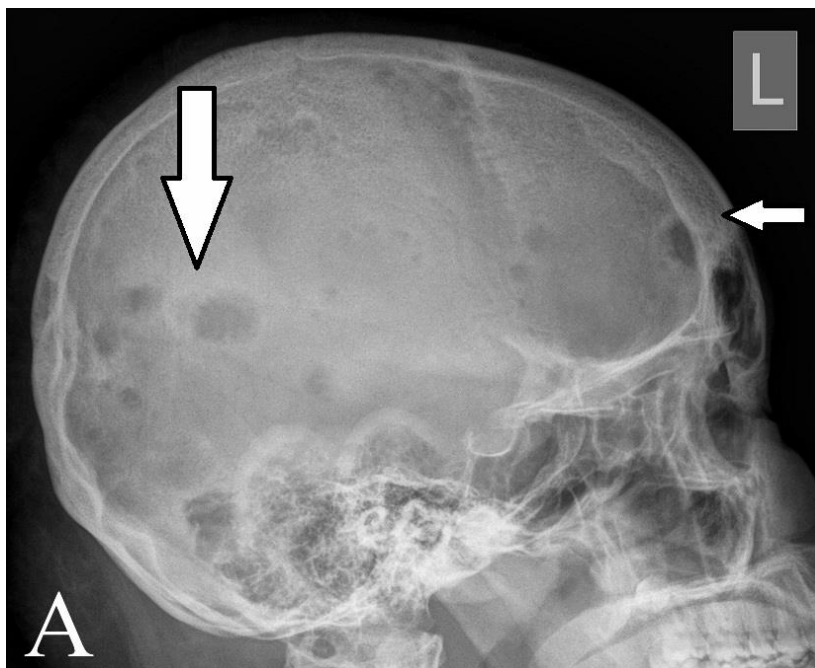


**Figure 10:** A 14 year old girl with Erdheim-Chester disease. Computed radiography image of skull, lateral view obtained after one year of Interferon alpha treatment shows stable osteolytic lesions of skull vault (arrows).

<b>Etiology</b>	A form of non-Langerhans cell histiocytosis
<b>Incidence</b>	Fewer hundreds of cases reported in literature
<b>Gender preference</b>	Male predominance in some series, but gender ratio not established due to its rarity
<b>Age</b>	Mean age 50 years
<b>Risk factors</b>	No specific risk factor
<b>Treatment</b>	Standard treatment not yet established. Interferon alpha is used with good results
<b>Prognosis</b>	At five years overall survival 41 percent.
<b>Imaging findings</b>	Bilateral symmetric osteosclerosis of diaphysis of long bones is nearly universal

**Table 1:** Summary table for Erdheim-Chester disease



Pathology	Plain radiographs	CT/MR	Histology
<b>Erdheim-Chester disease</b>	Bilateral symmetric diaphyseal osteosclerosis of long bones.	Intramedullary lesions with endosteal scalloping and high T2 signal of marrow.	Infiltration of lipid laden histiocytes. Touton-type giant cells. Immunohistochemistry reactivity to CD 68 and non-reactivity to S 100.
<b>Langerhans cell histiocytosis</b>	Osteolytic lesions in bones, less specific localization.	Cortical based osseous lesions and associated soft tissue component, but not specific.	Presence of typical Langerhans cells and positive immunohistochemical staining for CD1a and CD207. Birbeck granules on electron microscopy.
<b>Osteosclerotic myeloma with POEMS syndrome</b>	Less symmetric bone sclerosis. Less specific localization.	Sclerotic lesions in axial and appendicular skeleton with characteristic clinical features helps in its diagnosis	Bone marrow biopsy shows lambda-restricted monoclonal gammopathy, plasma cell rimming around lymphoid aggregates, and megakaryocytic hyperplasia.
<b>Paget's disease</b>	Less symmetric bone sclerosis. Less specific localization.	Expanded bones with cortical thickening and coarse trabecula are seen in blastic phase.	Abnormal bony architecture and presence of large osteoclasts.

**Table 2:** Differential diagnosis table for Erdheim-Chester disease

**ABBREVIATIONS**

ALL = Acute lymphoblastic leukemia  
 CT = Computed tomography  
 DM = Diabetes mellitus  
 MRI = Magnetic resonance imaging  
 POEMS = Polyneuropathy, organomegaly, endocrinopathy, monoclonal gammopathy and skin changes syndrome

**KEYWORDS**

Erdheim-Chester disease; Langerhans cell histiocytosis; osteolytic lesions; Touton type giant cells; Interferon alpha

**Online access**

This publication is online available at:  
[www.radiologycases.com/index.php/radiologycases/article/view/1899](http://www.radiologycases.com/index.php/radiologycases/article/view/1899)

**Peer discussion**

Discuss this manuscript in our protected discussion forum at:  
[www.radiolopolis.com/forums/JRCR](http://www.radiolopolis.com/forums/JRCR)

**Interactivity**

This publication is available as an interactive article with scroll, window/level, magnify and more features.  
 Available online at [www.RadiologyCases.com](http://www.RadiologyCases.com)

Published by EduRad



[www.EduRad.org](http://www.EduRad.org)